

AEOLIAN SEDIMENT TRANSPORT IN MARTIAN CRATERS. M. D. Day¹, W. Anderson², and G. A. Kocurek¹, ¹University of Texas at Austin, Department of Geological Sciences, 1 University Station C1100, Austin, TX 78712, *mdday@utexas.edu*, ²University of Texas at Dallas, Department of Mechanical Engineering.

Introduction: Aeolian erosion and deposition dominate the modern Martian landscape. As the primary sedimentary basins, craters are critical to understanding the modern Martian sediment budget. Layered sedimentary rocks have been identified in craters across Mars, particularly in the ancient southern highlands [1]. These deposits, including the mound currently traversed by the Mars Science Laboratory rover *Curiosity*, form a variety of morphologies hypothesized to represent a spectrum of erosional stages reduced from fully filled craters [1]. These interior layered deposits have been interpreted as both ancient lacustrine deposits [2], and as dust mounds deposited in place [3]. Yardangs, ventifacts, and dune fields observed in crater interiors provide evidence that aeolian erosion and deposition played at least some role in the evolution of these deposit morphologies. The goal of this work is to determine whether aeolian sediment transport could have been responsible for the range of crater interior morphologies observed on Mars today.

Methods: Initially, qualitative wind tunnel experiments were conducted to determine if the erosion patterns observed in previous works could be produced in laboratory-scale physical models [1]. Model craters made from an unerodable substrate were filled with fine sand, dampened for cohesion, and subjected to a unidirectional 7 m/s wind until all fill had been removed. At this wind speed, comparable to measured winds on Mars, erosional patterns similar to those observed on Mars changed the morphology of the interior

fill from filling the crater, to forming an initial moat around the interior of the rim, retreating to a central mound, isolated butte, and eventually emptying the crater [1]. Two crater models were used to represent end member geometries of complex craters (1:10 and 1:30 depth to diameter ratios) [4]. Both models yielded similar repeatable erosional morphologies. Encouraging results from these experiments motivated further more quantitative investigation.

Large eddy simulation (LES) was used to model flow over the two end member geometries also studied in the wind tunnel. With LES, five deflationary stages were considered for each end member, thus capturing key states of the erosional spectrum. Modeled crater topographies were formed using superimposed Gaussian curves. To reduce computational complexity, all crater topography sits above a base-level surrounding plain, and no negative topographic step is modeled (Fig 1a). LES subjected the craters to a unidirectional wind regime and predicted shear stress distributions across the crater domains. Although LES is not typically applied on Earth to systems as large as craters, the increased depth of the Martian atmospheric boundary layer relative to Earth suggests larger scale applications [5].

On Mars, once saltation has been initiated, it can be sustained at shear velocities an order of magnitude lower than the fluid threshold critical shear velocity [6]. Time averaged shear velocity distributions resulting from LES were compared with impact threshold

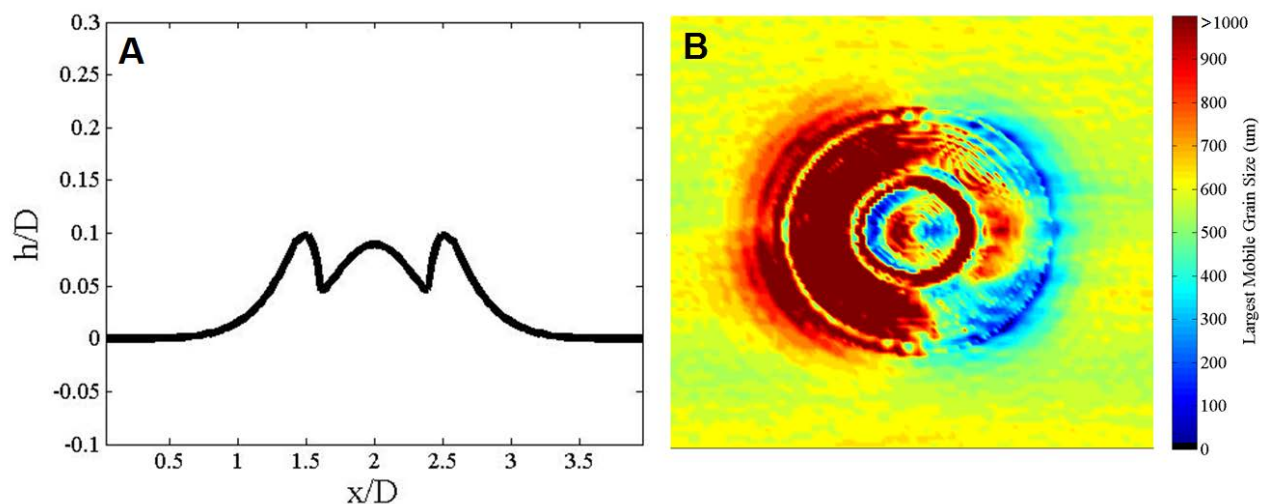


Figure 1: A) Cross sectional profile of an idealized crater topography used in LES. This model represents an intermediate stage of erosion of the interior deposit where an initial moat has been generated around the crater rim interior. The depth to diameter ratio of this model is 1:10, representing a small diameter end member of complex crater geometries. B) Plan-view of the same crater in A) with colors representing the largest mobile grain size throughout the domain calculated for 30 m/s winds. Wind is from left to right.

critical shear velocity curves to determine the largest mobile grain size across each of the ten modeled craters for a range of primary wind speeds (Fig 1b) [6]. Because interactions due to electrostatic forces are beyond the scope of this analysis, dust sized particles ($d < 50 \mu\text{m}$) are not considered.

A survey of Martian craters was conducted using Viking color and Context Camera (CTX) imagery to identify craters with interior morphologies undergoing active aeolian erosion and deposition. The survey was limited to plus and minus 60° latitude to limit the influence of ice on crater interior morphologies. Guided by existing surveys, 36 craters with interior layered deposits were identified with morphologies along the hypothesized erosional spectrum [7, 8, 1]. Additionally, 76 craters with active interior dune fields were identified. The low albedo of the dunes indicates an absence of dust mantling and suggests that these bedforms are actively migrating. High Resolution Imaging Science Experiment (HiRISE) imagery shows ripples superimposed on the stoss sides of barchan and crescentic dunes, and additional ripples in regions downwind where dune fields give way to sand sheets.

Associated with many of the observed craters are low albedo tails emanating from the craters (Fig 2). Inferring wind direction from slip faces in intra-crater dune fields, these tails are consistently located downwind of the crater, and elongated in the downwind direction. Previously suggested to be wind streaks, the dark material mantling the downwind plains is likely sourced from the similarly low albedo intra-crater dune fields [9].

Results: Using the largest mobile grain size as a proxy for transport potential, results from LES modeling indicate that sediment is most readily transported into craters and around their interior rims, but that only during high wind events can sediment leave the downwind end of the crater. This interpretation matches the observations of both layered crater interiors and interior dune fields. Intra-crater dune fields tend to be observed as terminal dune fields, trapped at the downwind interior of the crater near the crater rim. Individual dunes are not preserved as sediment is transported over the rim and out of the crater, but downwind dark wind streaks suggest that sediment is being excavated. It is hypothesized that sediment transported from the sheltered crater interior is thinly dispersed over the area of the wind streak in thicknesses too slight to form bedforms that could be resolved by HiRISE.

Though both end member geometries indicated on-ly limited transport out of craters, the 1:10 depth to diameter ratio models developed a downwind zone of increased transport relative to their 1:30 counterparts,

suggesting sediment is more easily excavated from smaller craters.

The regions of highest transport predicted by LES correspond with the regions of highest erosion in the hypothesized erosional spectrum. In addition to the patterns observed in wind tunnel experiments, LES generates zones of high shear stress around rim interiors that would cause erosion of any preexisting deposit, creating a positive feedback of erosion, and the spectrum hypothesized. The abundant yardangs hosted by many of the observed interior layered deposits support the interpretation of widespread aeolian erosion inferred from these results.

Results from this study indicate that craters on modern Mars function as temporary depo-centers, trapping sediment that then migrates across the crater to form dune fields and is eventually excavated during high wind events. Preexisting layered deposits in these craters could have been subjected to intense abrasion from trapped sediments, and slowly eroded to produce the range of morphologies observed today.

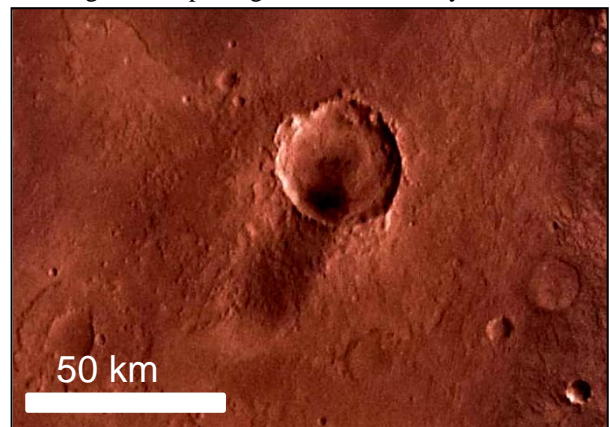


Figure 2: Viking color image of Coimbra crater showing its interior low albedo sandy deposit and downwind wind streak crater tail. Depth to diameter ratio is approximately 1:30

References: [1] Malin, M. C. and Edgett K. S. (2000) *Science*, 290, 1927-1937. [2] Grotzinger, J. P. et al. (2014) *Science*, 343, 1242777. [3] Kite E. S. et al. (2013) *Geology*, 41, 543-546. [4] Robbins, S. J. and Hynek B. M. (2012) *JRG*, 117, E06001. [5] Petrosyan, A. et al. (2011) *Rev. Geophys.*, 49, RG3005. [6] Kok J. F. (2010) *GRL*, 37, L12202. [7] DeLano K. and Hynek B. M. (2011) *LPSC XLII* Abstract # 2636. [8] Bennet, K. A. and Bell, J. F. III (2014) *LPSC XLV* Abstract # 1539. [9] Edgett K. S. and Malin M. C. (2000) *Geophys. R. Planets*, 105, 1623-1650.